The Electrochemical Behavior of Al Alloys in NaCl Solution in the Presence of Pyrazole Derivative

Grudić, Veselinka; Bošković, Ivana*+; Radonjić, Dragan; Jaćimović, Željko; Knežević, Bojana

Faculty of Metallurgy and Technology, University of Montenegro, Džordža Vašingtona bb, 81000 Podgorica, MONTENEGRO

ABSTRACT: *This paper studies the corrosion inhibition of Al-Mg alloy system in 0.5 mol/dm^3 NaCl solution in the presence of pyrazole derivative using potentiodynamic polarization and linear polarization method. The inhibition efficiency as a function of concentration and temperature was investigated. From the polarization curves, it can be concluded that the pyrazole derivative behaves like a mixed inhibitor. It has been shown that the efficiency of the inhibitor increases with increasing concentration and with increasing temperature and it indicates a chemisorption process. It was concluded that the pyrazole derivative adsorbed on the electrode blocks the active surface sites and reduces the corrosion rate. The kinetic and thermodynamic parameters of adsorption process were determined. The relatively low efficiency of the inhibitor at room temperature could be an indicator of increased desorption in the adsorption-desorption equilibrium process. With increasing temperature the equilibrium is shifted in the direction of adsorption, causing an increase in efficiency. Also, the positive values of equilibrium adsorption constant K_{ads} indicate chemisorption of the pyrazole derivative on the alloy surface. The values of the activation energy in the presence of inhibitor were lower than in the uninhibited solution, which also indicates the chemical adsorption. Negative values of adsorption free energy ΔG_{ads} show that the adsorption process is spontaneous.*

KEYWORDS: *Corrosion rate; Pyrazole derivative; Inhibition efficiency; Adsorption isotherms.*

INTRODUCTION

Beside their good qualities, technically pure aluminum can not satisfy the requirements in structural terms. In order to improve its characteristics, aluminum is alloyed with different elements (Cu, Si, Mg, Mn) [1]. In contact with air, aluminum, as a reactive metal, is covered spontaneously with an oxide layer that prevents further oxidation. It is dissolved in more concentrated solution of acids, alkalis or salts. The oxide film may be greatly destabilized in the presence of some of halide ions, especially chloride [2]**.** The main problem of Al and Al alloys corrosion is the local destruction of the passive film which causes pitting corrosion in the chloride solutions [3]. The corrosion effect of aggressive components in the electrolyte, in practice, is often reduced by using corrosion inhibitors. The organic inhibitors mostly form a film on the metal surface. The efficiency of organic corrosion inhibitors is increased if containing a polar functional group with S, O, or N atoms in the molecule,

***** *To whom correspondence should be addressed.*
+ E-mail ivabo@ac.me
1021-9986/2019/2/127-138 *12/$/6.02*

Table 1: Chemical composition of investigated aluminum alloy.

chemical element	Al	Mg	Zn	Cu	Mn	Fe	Si	Ti	Cr
wt %	base	6,92	0,724	0,3	0,284	0,26	0,146	0,13	0,185

heterocyclic compounds or π electrons. The examples of such organic inhibitors are amines, urea, aldehydes, heterocyclic nitrogen compounds, sulfur-containing compounds, as well as ascorbic acid, tryptamine, caffeine, and extracts of natural substances.

Very efficient corrosion inhibitors (chromate, polyphosphates, amines) are rarely used due to its negative effects on the environment. Therefore, in recent years, more attention is paid to the application of more environmentally friendly corrosion inhibitors like pyrazole. Pyrazoles are the part of the many drugs (especially of anti-pyretics and anti-rheumatics), herbicides and fungicides. This paper studies the efficiency of the pyrazole derivative as a corrosion inhibitor on aluminum alloy in the temperature range from 298K to 313K in 0.51mol/dm^3 NaCl solution.

EXPERIMENTAL SECTION

The chemical composition of the alloy, tested by non-destructive method on the X-RAY quantometer is shown in Table 1.

Investigation of corrosion behavior was carried out in the 0.51 mol/dm^3 NaCl solution in the presence of 4-acetyl-3 (5) -amino-5 (3) methylpyrazole as a corrosion inhibitor [4]. Pyrazole derivative is poorly soluble in water, but well soluble in ethanol. Therefore, a basic solution of the inhibitor (concentration of 0.6 mmol/dm^3) was prepared by dissolving the pyrazole derivative in ethanol. A series of solutions in the concentration range 0.1 - 0.6 mmol dm^{-3} were made by dilution of the basic inhibitor solution with aqueous NaCl (0.5 mol/dm^3). Pyrazole (1,2 diazole) belongs to the group of azoles. A five- membered ring composed of three carbon atoms and two nitrogen atoms so-called nitrogen "pyridine" and nitrogen "pyrrole" type. The nitrogen atoms may change the "role" so that the pyrazole ring is characterized by apparent tautomeria.

Due to the presence of the "pyridine" nitrogen atoms, pyrazole and its derivatives are known as good ligands. Namely, in contrast to the pyrrole nitrogen atom which is, in terms of coordination, a fairly non-reactive, the pyridine nitrogen is subjected to electrophilic attack which allows its binding to metal ions (Fig. 1).

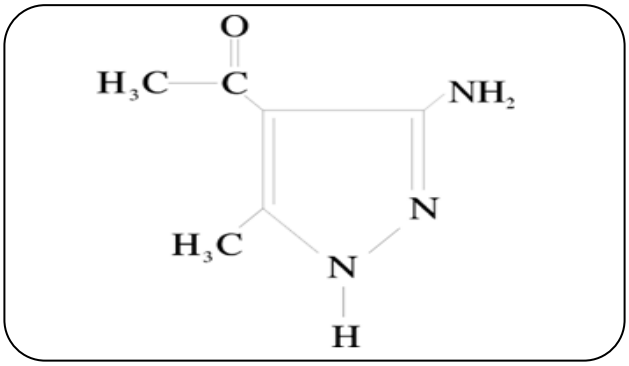

Fig. 1: The structural formula of 4-acetyl 3- (5) -amino-5 (3) methylpyrazole.

Corrosion investigations were done by Potentiostate-Galvanostate 273 analyzer model PAR – 325II interfaced with software and computerized laser printer.

Polarization experiments (potentiodynamic polarization method and linear polarization method) were carried out in a special three-electrode glass cell with a graphite counter electrode of cylindrical shape and a saturated calomel electrode (SCE) as reference. The working electrode in a disk shape made of Al alloy (whose composition is given in Table 1) is placed in an appropriate carrier, such that only one side of the disc surface (1cm^2) was exposed to the electrolyte. Before the measurement the surface of the working electrode was mechanically cleaned with abrasive sanding papers of fineness 600 and 1200, then washed with a stream of redistilled water and ultrasonically degreased in ethanol, after which it was The working electrode was immersed in a test solution for 30 min to establish a stable value of open circuit potential, followed by measuring the polarization resistance in the range of potential ± 20 mV compared to the open circuit potential at a scan rate of 1 mV/s. Potentiodynamic curves were recorded in the potential range of ± 150 mV compared to the open-circuit potential at polarization rate of 1 mV/s.

RESULTS AND DISSCUSION

Investigation of inhibition efficiency

In order to determine the optimal working concentration of the tested pyrazole derivative, as well as

Table 2: Electrochemical polarization parameters for aluminum alloy in 0.51 mol dm^{-3} NaCl solution in the presence of various concentrations of pyrazole derivative.

$C_{pyrazole}$ [mmol/dm^3]	j_{corr} [μA/cm^2]	E_{corr} [mV]	b_c [mVdec]	b_a [mV/dec]	η [%]
0	2.88	-832.2	100	100	
0.1	2.512	-823	86.38	89.52	12.78
0.15	2.344	-820	74.95	61.43	18.61
0.3	1.995	-814.1	86.33	47.43	32.11
0.4	1.778	-813.5	92.91	78.70	38.23
0.6	1.259	-812.6	89.88	76.34	56.28

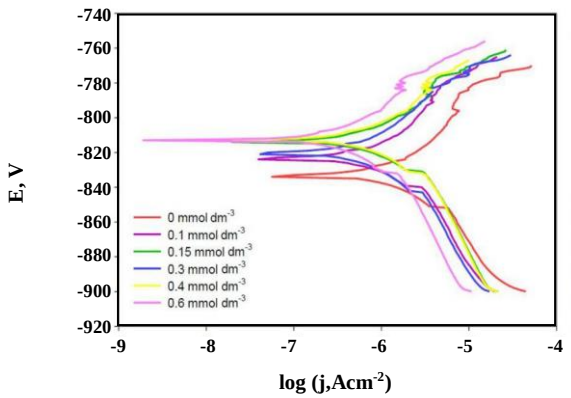

Fig. 2: Potentiodynamic polarization curves of Al alloy in 0.51 mol/dm^3 NaCl solution as a function of various concentrations of the pyrazole derivative at 298K.

the dependence of the inhibition efficiency in a function of concentration, polarization measurements were performed in NaCl solutions with concentration of pyrazole derivative from $1\cdot10^{-4}$ mol/dm^3 to $6\cdot10^{-4}$ mol/dm^3 at 25 °C.

Potentiodynamic polarization curves of Al alloy in 0.51 mol/dm^3 NaCl solution as a function of various concentrations of the pyrazole derivative are shown in Fig. 2. The values of polarization parameters such as corrosion current density, corrosion potential, anodic and cathodic Tafel slopes, and inhibition efficiency are given in Table 2.

Cathodic and anodic current densities were reduced by shifting corrosion potential to more positive values (Fig. 2). Generally, if the displacement in corrosion potential is more than 85 mV in the presence of inhibitor with the respect to corrosion potential of the blank, the inhibitor can be classified as a cathodic or anodic type [5]. No significant changes in corrosion potentials (Table 2) with pyrazole derivative compared to blank suggest mixed type of inhibitor with a more pronounced impact on the anode reaction [6, 7, 8].

Based on data from Table 2 it can be observed that the reduction of the corrosion current density in the presence of pyrazole derivative with increasing concentration of the inhibitor is a result of its adsorption on the aluminum alloy surface [6]. The inhibition efficiency was calculated using the equation (1):

$$\eta(\%) = \left(\frac{j^{o}_{corr} - j_{corr}}{j^{o}_{corr}} \right) \times 100 \qquad (1)$$

where j_{corr} and j^{o}_{corr} are the values of corrosion current density with and without inhibitor respectively.

The number of active sites was reduced by adsorption of pyrazole derivative on the alloy surface causing increase inhibitor efficiency with increasing its concentration in solution (Table 2)

The values of Tafel cathodic and anodic slopes (b_c, b_a) were slightly changed in solutions with various concentrations of pyrazole derivative. It means that there is no change in the mechanism of cathodic and anodic reaction in the presence of the inhibitor. Inhibitor activity can be explained by its simple adsorption on the electrode surface and by blocking active sites on the surface, which results in the reduction of corrosion rate.

In general, the adsorption of inhibitor on the interface of two phases leads to differences in the concentrations of inhibitors on the metal surface and in the solution. This process takes place until the equilibrium between the concentration of inhibitor in the solution and its concentration on the metal surface is achieved.

Adsorption of the inhibitor can influence the corrosion rate in two different ways:

Table 3: Corrosion parameters of Al alloy in 0,51 mol/dm³ NaCl in the presence of various concentrations of pyrazole derivative determined by polarization resistance method.

$C_{pyrazole}$ [mmol/dm³]	j_{corr} [μA/cm²]	R_p [kΩ]	θ	η [%]
0	2,902	7,483		
0,1	2,594	8,37	0,1059	10,59
0,15	2,530	8,584	0,1283	12,83
0,3	1,953	11,12	0,3271	32,71
0,4	1,748	12,42	0,3975	39,75
0,6	1,227	16,24	0,5322	53,22

- Reduction of the reaction area on the surface of the corroding metal (so-called geometric blocking effect)
- Change in activation energy of cathode and / or anode reaction in case of the inhibited corrosion process.

It is difficult to distinguish two aspects of the inhibitor activity of organic inhibitors. In theory, a constant value E_{corr} after the addition of the corrosion inhibitor indicates that the geometric effect is stronger than the effect of activation energy [5]. The evaluated values of E_{corr} after addition of pyrazole (Table 2) show the presence of both effects.

The values of the corrosion current density, polarization resistance and inhibition efficiency determined by polarization resistance method are shown in Table 3.

Since theoretical electrochemistry assumed that the reciprocal value of the polarization resistance is proportional to the corrosion rate, degree of surface coverage (θ) and the inhibition efficiency (η) are calculated according to the equation (2) [10]:

$$\eta = \theta \times 100 = \left(\frac{\left(R_p\right)_{inh} - R_p}{\left(R_p\right)_{inh}} \right) \times 100 \qquad (2)$$

Where R_p, $\left(R_p\right)_{inh}$ are the values of polarization resistance in the absence and in the presence of inhibitor respectively.

The values of polarization resistance (R_p) increase from 7,483 kΩ (in solution without pyrazole) to 16,24 kΩ (in $6 \cdot 10^{-4}$ mmol/dm³ pyrazole solution) indicating an increase of inhibition efficiency. The values of corrosion currents and the values of inhibition efficiencies are close to its values obtained by potentiodynamic method.

Activation energy and thermodynamic parameters of the inhibition process

The effect of temperature on the corrosion rate of aluminum alloy in NaCl solution was studied in the temperature range from 298 to 313 K. The values of corrosion parameters: the corrosion current density j_{corr}, inhibition efficiency η (%) and degree of surface coverage (θ) obtained by potentiodynamic method at various concentrations of inhibitor in a given temperature range are listed in Table 4.

The values of the corrosion current density (Table 4) are increased with temperature in the absence and in the presence of the inhibitor, but the increase was more pronounced in the absence of inhibitor, resulting into the increase of inhibition efficiency with rising temperatures. It may be explained by desorption and adsorption of inhibitor molecules that take place continuously at the metal surface. With increased temperature, equilibrium between these two opposing processes is shifted in the direction of the adsorption inhibitor molecules on the alloy surface [8, 9]. Increasing the inhibition efficiency with rising temperature can be explained by the formation of coordination bonds i.e. by the fact that the adsorption of pyrazole derivative on the Al alloy surface is dominantly chemisorption [8].

A quantitative relationship between temperature and the corrosion rate is given by Arrhenius′s equation:

$$j_{corr} = A \exp\left(-\frac{E_A}{RT} \right) \qquad (3)$$

where: j_{corr} is current density which is directly proportional to the corrosion rate, A is the Arrhenius′s pre-exponential factor, E_A is the apparent activation energy, R is the universal gas constant (8,314 J/K.mol),

Table 4: Corrosion parameters of Al alloy in 0.51 mol/dm³ NaCl in the absence and in the presence of the inhibitor at different temperatures.

C, [mmol/dm³]	T=298K			T=303K			T=308K			T= 313K		
	j_{corr} [μA/cm²]	θ	η [%]	j_{corr} [μA/cm²]	θ	η [%]	j_{corr} [μA/cm²]	θ	η [%]	j_{corr} [μA/cm²]	θ	η [%]
0	2.88	/	/	4.30	/	/	6.15	/	/	9.12	/	/
0.1	2.512	0.1278	12.78	3.49	0.1883	18.83	4.38	0.2878	28.78	6.32	0.3070	30.70
0.15	2.344	0.1861	18.61	3.14	0.2093	20.93	3.75	0.3902	39.02	5.23	0.4265	42.65
0.3	1.995	0.3211	32.11	2.44	0.4325	43.25	2.86	0.5349	53.49	3.38	0.6293	62.93
0.4	1.778	0.3823	38.23	2.1	0.5116	51.16	2.32	0.6228	62.28	2.85	0.6875	68.75
0.6	1.259	0.5628	56.28	1.46	0.6605	66.05	1.67	0.7284	72.84	1.95	0.7861	78.61

Table 5: The parameters of Arrhenius's linear dependence ln j_{corr} – 1/T in 0.51 mol dm⁻³ NaCl at various concentrations of pyrazole derivative

C [mmol/dm³]	R^2	E_A [kJ/mol]	A [μA/cm²]
0	O,9995	57,112	$3{,}02\cdot10^{10}$
0.1	0,989	38,021	$1{,}22\cdot10^{7}$
0.15	0,9954	34,411	$2{,}6\cdot10^{6}$
0.3	0,9985	25,974	$7{,}26\cdot10^{4}$
0.4	0,9911	23,379	$2{,}22\cdot10^{4}$
0.6	0,9952	21,915	$8{,}88\cdot10^{3}$

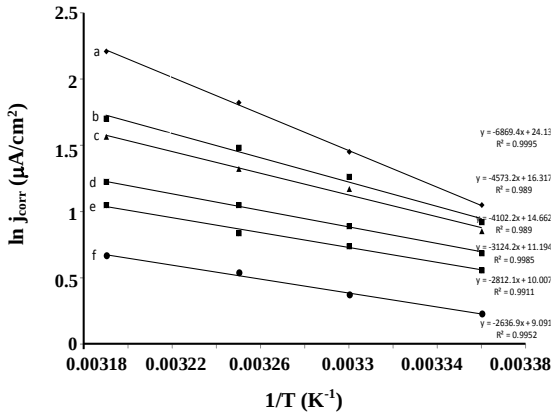

Fig. 3: Arrhenius's plots of ln j_{corr} versus 1/T for Al alloy in 0,51 mol/dm⁻³ NaCl solution at various concentrations of pyrazole derivative: (a) 0; (b) 0.1; (c) 0.15; (d) 0.3; (e) 0.4 and (f) 0.6 mmol dm⁻³

T is the absolute temperature (K). A plot of ln j_{corr} versus 1/T for 0.51 mol/dm³ NaCl solution without and with inhibitor were presented in Fig. 3. Obtained straight lines have a slope ($-E_A/R$) and intercept of lnA from which E_A and A were calculated and then listed in Table 5.

All of the correlation coefficients (R^2) show the values close to the unit which indicates that the corrosion of the Al alloy in 0.5 mol/dm³ NaCl solution is well described by Arrhenius's equation (Fig. 3)

The results presented in Table 5 show that the values of E_A are lower in the presence of corrosion inhibitor than those obtained in the inhibitor free solution and decreased with increasing inhibitor concentration. It points out the chemisorption of the pyrazole derivative molecules on the alloy surface [13,14].

Based on the results of polarization measurements at different temperatures and different concentrations of inhibitors, the two important kinetic parameters of corrosion were also calculated: activation enthalpy (ΔH_a^0) and activation entropy (ΔS_a^0) using the equation of transition state [15]:

$$j_{corr} = \frac{RT}{Nh}\exp\left(\frac{\Delta S^o_{ads}}{R}\right)\exp\left(\frac{\Delta H^o_{ads}}{RT}\right) \quad (4)$$

Where: N is Avogadro's number, and h is the Planck's constant.

Table 6: Thermodynamic parameters of the corrosion in 0.51 mol dm^{-3} NaCl solution at various concentrations of pyrazole derivative

C [mmol/dm^3]	R^2	ΔH_{ads}^0[kJ/mol]	ΔS_{ads}^0[J/mol.K]	ΔG_{ads}^0 [kJ/mol]
0	0.9954	43.148	-71.908	
0.1	0.9993	34.694	- 101.64	- 28.016
0.15	0.9950	28.87	-118.75	- 28.114
0.3	0.9902	19.381	-155.83	- 28.198
0.4	0.9917	16.996	-164.83	- 28.151
0.6	0.9910	1.523	-173.74	- 28.961

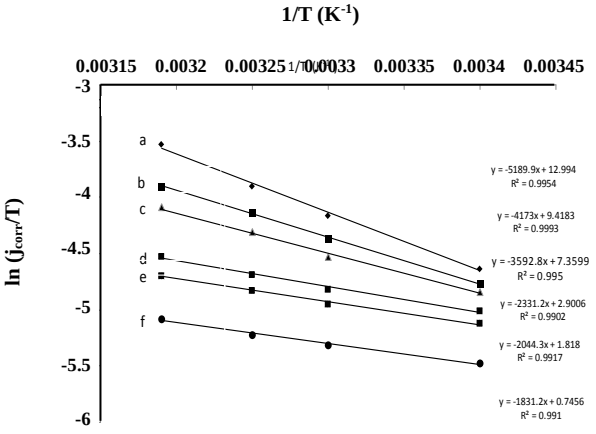

Fig. 4: A plot of ln (j_{corr}/T) versus 1/T in 0,51 mol dm^{-3} NaCl solution at various concentrations of pyrazole derivative: (a) 0; (b) 0.1; (c) 0.15; (d) 0.3; (e) 0.4 and (f) 0.6 mmol/dm^3.

A plot of ln (j_{corr}/*T*) versus 1/*T* is the straight line with the slope ($-\Delta H_{ads}^0/R$) and intercept [(ln (*R*/*Nh*)) + (ΔS_{ads}^0 /*R*)] (Fig.4). Kinetics parameters of the corrosion in NaCl solution in the absence and in the presence of pyrazole derivative are presented in Table 6.

The values of activation enthalpy ΔH_{ads}^0 are positive in all systems (Table 6) but they are lower in the presence of pyrazole derivative as well as they are continuously decreasing with increased concentration of inhibitor. The positive values of activation enthalpy reflect the difficult dissolution of the Al alloy in investigated solution [16]. High negative values of the activation entropy (ΔS_{ads}^0) both in the absence and in the presence of pyrazole indicate formation of the activated complex in the rate determining step represents an association rather than a dissociation step, meaning that a decrease in disorder takes place during the course of the transition from reactants to activated complex [8, 17,18].

The values of the adsorption free energy can be calculated using the Equations (5) and (6). Based on these values the applicability of specific isotherm can be estimated.

$$\Delta G_{ads} = -2.303RT\log(55.5K) \quad (5)$$

$$K = \frac{\theta}{\left[(1-\theta)C\right]} \quad (6)$$

where R is the gas constant, T is the absolute temperature, C is the inhibitor concentration; the value of 55,5 mol/dm^3 is water concentration, θ is the degree of surface coverage.

The obtained negative values of ΔG_{ads} (Table 7) characterize the spontaneity of the adsorption process under the used experimental conditions. Generally, values of ΔG_{ads} up to -20 kJ/mol are consistent with the electrostatic interaction between the charged molecules and the charged metal (physical adsorption), while those more negative than −40 kJ mol^{-1} involve charge sharing or charge transfer from the inhibitor molecules to the metal surface to form a coordinate type of bond (chemisorption) [19].

The values of ΔG_{ads} indicate that the pyrazole derivative adsorption on the alloy surface is mixed type, and includes two types of interaction: physisorption and chemisorption. In fact, the adsorption of organic molecules is not only a physical or chemical process [20]. In addition, it is generally accepted that, prior to chemisorption, the molecules are physically adsorbed, in the precursor state, on the metal surface [21]. The same adsorption mechanism was also observed in case of inhibition by pyrazole derivatives on the mild steel in HCl [6] and H_2SO_4 solution [7].

Table 7: The values of the adsorption free energy on the Al alloy surface.

C [mmol/dm³]	$-\Delta G_{ads}$ [kJ/mol]			
	298K	303K	308K	313K
0		/	/	/
0.1	28.016	29.645	31.582	32.450
0.15	28.114	29.594	31.691	32.637
0.3	28.198	29.873	31.472	32.952
0.4	28.151	29.950	31.565	32.765
0.6	28.961	30.488	31.799	33.211

Adsorption isotherms and adsorption parameters

The process of inhibition of metal corrosion is based on the adsorption of organic inhibitor molecules on the metal surface. In order to gain more information about the mode of pyrazole derivative adsorption on the alloy surface, the experimental data have been tested with several adsorption isotherms.

In theory, the adsorption process can be considered as substitution of x water molecules adsorbed on the metal surface with inhibitor molecules according to the following reaction [19]:

$$I_{(aq)} + xH_2O_{(ads)} \leftrightarrow I_{(ads)} + xH_2O_{(aq)} \quad (6)$$

Where $I_{(aq)}$ and $I_{(ads)}$ are organic inhibitor molecules in solution and organic inhibitor molecules adsorbed on the metal surface; $H_2O_{(ads)}$ represents the water molecules on the metal surface; x is the number of water molecules substituted with one inhibitor molecule.

The results obtained by the potentiodynamic method in the temperature range 298 - 313 K (Table 4) were used to calculate the adsorption isotherm parameters. The various isotherms (Langmuir′s, Temkin′s, El-Awady′s, Freundlich′s, Temkin′s and Adejo-Ekwenchi′s) were examined and they are shown by the following equations [23 -25]:

$$\text{Langmuir's isotherm} \quad \frac{C}{\theta} = \frac{1}{Kads} + C \quad (7)$$

$$\text{Freundlich's isotherm} \quad \log\theta = \log K_{ads} + n\log C \quad (8)$$

$$\text{Temkin's isotherm} \quad \theta = -\frac{2.303\log K_{ads}}{2a} - \frac{2.303\log C}{2a} \quad (9)$$

$$\text{El} - \text{Awady's isotherm} \quad (10)$$

$$\log\left(\frac{\theta}{1-\theta}\right) = \log K_{ads} + y\log C$$

$$\text{Adejo} - \text{Ekwenchi's isotherm} \quad (11)$$

$$\log\left(\frac{1}{1-\theta}\right) = \log K_{ads} + b\log C$$

Where K_{ads} is the equilibrium constant of adsorption process; θ is the degree of the surface coverage; C is the inhibitor concentration; a is a parameter whose value indicates the repulsion or attraction of adsorbate molecules.

The mentioned isotherms for the pyrazole adsorption are shown in Fig. 5, and corresponding parameters of the adsorption process are presented in Table 8.

Many adsorption isotherms were plotted, but the values of regression coefficients (R^2) confirmed that the adsorption of inhibitor follows Langmuir′s isotherm. The considerable deviation of the slope from the unit indicated that this isotherm could not be strictly applied. It has been postulated in the derivation of Langmuir′s equation that adsorbed molecules did not interact with one another, but this was not true in the case of the molecules having polar atoms or groups which could be adsorbed on the metal surface. Such adsorbed molecules interact by mutual repulsion or attraction and would affect the slope. The deviation of the slope could also be interpreted due to the changes in adsorption heat with increasing surface coverage [21, 26].

Therefore, experimental results have been fitted into the modified form of Langmur′s isotherm known as El-Awady′s isotherm. The reciprocal value of the parameter **y** represents the number of water molecules substituted with one molecule of the inhibitor [27]. The values of

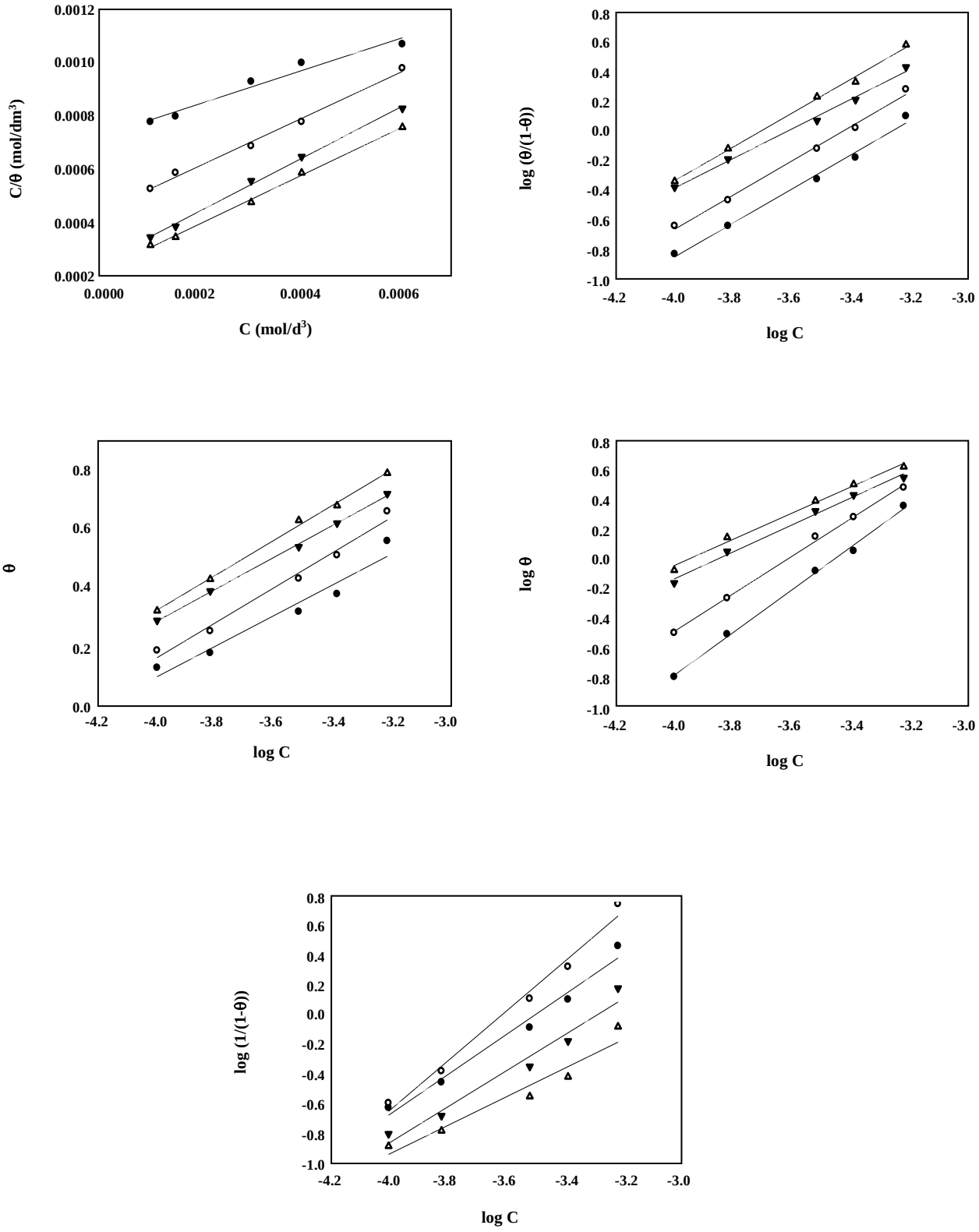

Fig. 5: Isotherm plots for the pyrazole derivative adsorption on aluminium alloy surface at different temperatures: (a) Langmuir; (b) El-Awady; (c)Temkin, (d) Freundlich and (e) Adejo-Ekwenchi isotherm (●-298K; o - 303K; ▼- 308K; ▲-313K).

Table 8: Adsorption parameters for using isotherms.

Isotherm	T[K]	R^2	K		$-\Delta G_{ads}$
Langmuir	298	0.9654	1428.57		27.954
	303	0.9936	2500.00		29.833
	308	0.9974	3333.33		31.062
	313	0.9976	50000		32.621
				n	
Freundlich	298	0.9970	208.40	0.8008	23,183
	303	0.9978	125.49	0.7046	22,285
	308	0.9926	31.769	0.5062	18,743
	313	0.9916	31.052	0.4912	19,395
El-Awady				y	
	298	0.9911	5970,35	1.1563	31.947
	303	0.9947	9878,71	1.1644	33,295
	308	0.9943	4377.24	1.0065	31.759
	313	0.9964	18569,49	1,1512	36.056
Temkin				a	
	298	0.9461	15473.91	-2.1992	33.858
	303	0.9834	18780.19	-1.9224	34.914
	308	0.9987	33814.27	-2.1121	36.996
	313	0.9970	34930.11	-1.9239	37.681
Adejo- Ekwenchi				b	
	298	0.9394	33.29	0.3737	18.638
	303	0.9654	86.72	0.4705	21.363
	308	0.9859	550.55	0.6504	26.473
	313	0.9792	167.65	0.5238	23.784
	298	0.9654	1428.57		27.954

this parameter (0.8648, 0.8588, 0.9935 and 0.8687 at 298, 303, 308 and 313K respectively) are close to the unit, which indicates that one water molecule is replaced by one molecule of adsorbed inhibitor. Parameter Freundlich′s isotherm (Table 8) i.e. the average value (n = 0.6257) close to the typical value of 0.6 [28], as well as a high value of R^2, indicating that the adsorption may be described by Freundlich′s adsorption isotherm. However, the value of ΔG_{ads} obtained from this isotherm is lower than the value obtained by conventional manner (Table 6). Therefore, pyrazole adsorption on the Al alloy cannot be modeled by Freundlich′s isotherm.

Temkin′s isotherm is applicable to the chemisorption process and indicates that uncharged molecules react with a heterogenous surface. The negative values of the molecular interaction parameters ″a″ are an indicator of the participation of molecular species in the adsorption process [29]. Based on the following facts: the value of R^2 is close to the unit, the molecules of the pyrazole derivative were adsorbed on the alloy′s surface by chemisorption and the values of ΔG_{ads} obtained from these isotherms are close to the values obtained by a conventional manner (Table 5), it can be concluded that the pyrazole derivative adsorption could be described by Temkin′s isotherm.

Table 9: Standard thermodynamic parameters of pyrazole derivative adsorption on the Al alloy surface in 0,51 mol/dm³ NaCl solution at different temperatures.

T [K]	ΔG^0_{ads} [kJ/mol]	ΔH^0_{ads} [kJ/mol]	ΔS^0_{ads} [J/K.mol]
298	-33.858	33,817	227,097
303	-34.914	33,817	226,835
308	-36.996	33,817	229,912
313	-37.681	33,817	228,428

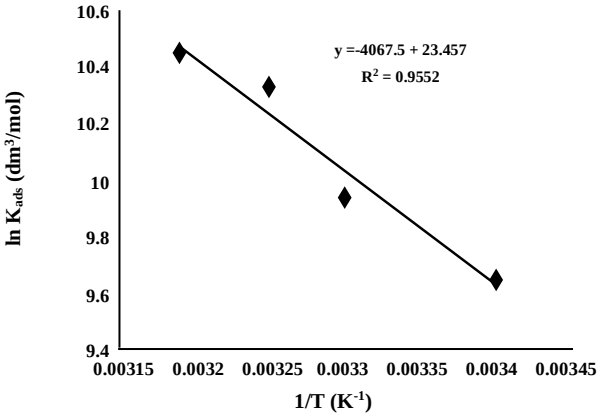

Fig. 6: A plot ln K_{ads} versus 1/T for pyrazole derivative adsorbed on the Al alloy surface in NaCl solution.

The use of the newly proposed Adejo-Ekwenchi′s isotherm can resolve ambiguity association with the characterization of adsorption behavior of inhibitor. The ″b″ parameter clearly shows whether the adsorption process is physisorption or chemisorption [25]. The value of ″b″ for the adsorption of pyrazole increases with rise in temperature signifying chemisorption process.

As previously noted, the increase in the inhibition efficiency with increased temperature as well as reducing of apparent activation energy in the presence of pyrazole derivative, indicate that the adsorption is predominantly a chemical process, followed by physisorption. Also, ΔG_{ads} values decrease with increasing temperature, additionally confirm that the inhibitor at higher temperatures show a greater tendency to the adsorption on the surface of Al alloy.

Correlation between standard free energy, standard enthalpy and standard entropy for adsorption process is given by the equation:

$$\Delta G^0_{ads} = \Delta H^0_{ads} - T\Delta S^0_{ads} \quad (12)$$

Based on the temperature dependence of the constant of adsorption, the value of ΔH^0_{ads} is calculated using Van't Hoff equation:

$$\ln K_{ads} = -\frac{\Delta H^0_{ads}}{RT} + \text{const} \quad (13)$$

The values of standard adsorption enthalpy ΔH^0_{ads} were calculated from the slope of the plot ln K_{ads} versus 1/T (Fig. 6). The standard adsorption entropies were calculated by using Equation (12). The values of these thermodynamic parameters are presented in Table 9.

Positive values of ΔH^0_{ads} indicate that the adsorption process of the pyrazole derivative is endothermic and complex, dominantly chemical process. Positive values of ΔS^0_{ads} can be explained by the fact that the adsorption of the inhibitor molecules is followed by desorption of water molecules from the surface of the alloy. Thermodynamic values of ΔS^0_{ads} are the algebraic sum of those of the adsorption of inhibitor molecules and the desorption of the water molecules. Therefore, the positive values of entropy can be attributed to the increase in solvent entropy [30, 31].

CONCLUSIONS

The results in this paper confirmed that pyrazole derivative can be used as a corrosion inhibitor for Al-Mg alloy in NaCl solution. The corrosion current decreases and the polarization resistance increases with risen inhibitor concentration, indicating corrosion rate decrease. Based on the changes in corrosion potential in the presence of inhibitor as compared to the corrosion potential in NaCl solution without inhibitor, pyrazole derivative can be classified as a corrosion inhibitor of the mixed type. Minor changes in the value of Tafel anodic and cathodic slopes indicate that there is no change in the mechanism of the anodic and cathodic reaction in the presence of pyrazole derivative. Therefore, inhibition

the activity can be explained by simple inhibitor adsorption on the electrode surface and by blocking the active sites on the surface which cause the corrosion rate reduction.

The increase of the inhibition efficiency with increased temperature as well as the values of the apparent activation energy, values of the standard free energy of adsorption and the values standard adsorption enthalpy indicate that the adsorption of the pyrazole derivative is a complex, dominantly chemical process. The obtained results show that this process could be described by modified form of Langmur′s isotherm, Temkin′s isotherm and Adejo-Ekwenchi′s isotherm.

Received : Nov. 6, 2017 ; Accepted : Mar. 12, 2018

REFERENCES

[1] Davis J.R., "Corrosion of Aluminum and Aluminum Alloys", 1st ed.; ASM International: Materials Park, OH, USA, 1999.

[2] Hasenay D., Seruga M., The Growth Kinetics and Properties of Potentiodynamically Formed Thin Oxide Films on Aluminum in Citric Acid Solutions, *J. Appl. Electrochem.*, **37**: 1001–1008 (2007).

[3] Abdel Rehim S.S., Hassan H.H., Amin M.A., Chronoamperometric Studies of Pitting Corrosion of Al and (Al–Si) Alloys by Halide Ions in Neutral Sulphate Solutions, *Corros. Sci.*, **46** (8): 1921–1938 (2004).

[4] Jaćimović Ž.K., Latinović N., Bošković I. and Tomić Z., The Influence of a Newly Synthesized Zn(II) and Cu(II) Complexes based on Pyrazole Derivatives on the Inhibition of Phomopsis Viticola Sacc.(Sacc.) under Laboratory Conditions, *Res. J. Chem. Environ.*, **17**(10): 23-27(2013)

[5] Wang Z., The Inhibition Effect of Bis-Benzimidazole Compound for Mild Steel in 0.5 M HCl Solution, *Int. J. Electrochem. Sci.*, **7**: 11149–11160 (2012).

[6] Louadi Y.E., Abrigach F., Bouyanzer A.,Touzani R., El Assyry A., Zarrouk A., Hammouti B., Theoretical and Experimental Studies on the Corrosion Inhibition Potentials of Two Tetrakis Pyrazole Derivatives for Mild Steel in 1.0 M HCl, *Port. Electrochim. Acta*, **35(3)**: 159-178 (2017).

[7] EL Arouji S., Alaoui Ismaili K., Zerrouki A., El Kadiri S., Rais Z., Filali Baba M.,Taleb M., Emran K.M., Zarrouk A., Aounit A., Hammouti B., Inhibition Effects of a New Syntheses Pyrazole Derivative on the Corrosion Ofmild Steel in Sulfuric Acid Solution, *Der Pharma Chemica*, **7(10)**: 67-76 (2015).

[8] Abdel Hameed R.S., Al-Shafey H. I., Abul Magd A.S., Shehata H.A., Pyrazole Derivatives as Corrosion Inhibitor for C- Steel in Hydrochloric Acid Medium, *J. Mater. Environ. Sci.*, **3**(2): 294-305 (2012).

[9] Ahamad W.I., Prasad R., Quraishi M.A., Inhibition of Mild Steel Corrosion in Acidic Solution by Pheniramine Drug: Experimental and Theoretical Study, *Corros. Sci.*, **52**: 3033–3041 (2010).

[10] Halambek J., Bubalo M.C., Redovniković I.R., Berković K., Corrosion Inhibition of AA 5052 Aluminum Alloy in NaCl Solution by Different Types of Honey, *Int. J. Electrochem. Sci.*, **9**: 5496 (2014).

[11] Yadav M., Kumar S., Behera D., Bahadur I., Ramjugernath D., Electrochemical and Quantum Chemical Studies on Adsorption and Corrosion Inhibition Performance of Quinoline-Thiazole Derivatives on Mild Steel in Hydrochloric Acid Solution, *Int. J. Electrochem. Sci.*, **9**: 5235–5257 (2014).

[12] Fragoza - Mar L., Olivares-Xometl O., Domínguez - Aguilar M.A., Flores E.A., Arellanes-Lozada P., Jimenez-Cruz F., Adsorption Properties and Inhibition of C38 Steel Corrosion in Hydrochloric Solution by Some Indole Derivates: Temperature Effect, Activation Energies and Thermodynamics of Adsorption, *Corros. Sci.*, **61**: 171–184 (2012).

[13] Behpour M., Ghoreishi S. M., Soltani N., Salavati- Niasari M., Hamadanian M. and Gandomi A., Electrochemical and Theoretical Investigation on the Corrosion Inhibition of Mild Steel by Thiosalicylaldehyde Derivatives in Hydrochloric Acid Solution, *Corros. Sci.*, **50**(8): 2172-2181 (2008).

[14] Wang X., Wang Y.g, YGu, Y.M.A, F. Hi S., Nui W., Wang Q., Inhibition and Adsorptive Behavior of Synthesized 1,4-bis (2-benzimidazolyl) Benzene on Mild Steel in 3 M HCl Solution, *Int. J. Electrochem. Sci.*, **9:** 1840–1853 (2014).

[15] Yadav M., Kumar S., Behera D Bahadur,Deresh Ramjugernath I., Electrochemical and Quantum Chemical Studies on Adsorption and Corrosion Inhibition Performance of Quinoline-Thiazole Derivatives on Mild Steel in Hydrochloric Acid Solution, *Int. J. Electrochem. Sci*., **9**: 5235 -5257 (2014).

[16] Singh A.K., Quraishi M.A., Effect of Cefazolin on the Corrosion of Mild Steel in HCl Solution, *Corros. Sci*. **52**: 152–160 (2010).

[17] Fu J., Pan J., Liu Z., Li S., Wang Y., Corrosion Inhibition of Mild Steel by Benzopyranone Derivative in 1.0 M HCl Solutions, *Int. J. Electrochem. Sci*., **6**: 2072–2089 (2011).

[18] Ramesh S.V., Adhikari V., Electrochemical and Quantum Chemical Studies on Adsorption and Corrosion Inhibition Performance of Quinoline - Thiazole Derivatives on Mild Steel in Hydrochloric Acid Solution, *Bull. Mater.Sci*., **31**: 699−711 (2007).

[19] Doner A., Solmaz R., Ozcan M., Kardas G., Experimental and Theoretical Studies of Thiazoles as Corrosion Inhibitors for Mild Steel in Sulphuric Acid Solution, *Corros. Sci*., **53**: 2902–2913 (2011).

[20] Wang F.P., Kang W.L., Jin H.M., "Corrosion Electrochemistry Mechanism, Methods and Applications, Chemical Industrial Engineering Press", Beijing, China (2008).

[21] Oguzie E.E., Okolue B.N., Ebenso E.E., Onuoha G.N., Onuchukwu A.I., Evaluation of the Inhibitory Effect of Methylene Blue Dye on the Corrosion of Aluminium in Hydrochloric Acid, *Mater. Chem. Phys*., **87**: 394–401 (2004).

[22] Zarrouk A., Warad I., Hammouti B., Dafali A., Al-Deyab S.S., Benchat N., The effect of Temperature on the Corrosion of Cu/HNO_3 in the Presence of Organic Inhibitor: part-2, *Int. J. of Electrochem. Sci*., **5**(10): 1516–1526 (2010).

[23] Arenos M.A., Bethencourt M., Botana F.G., Domborenena J., Marcos M., Inhibition of 5083 Aluminum Alloy and Galvanised Steel by Lanthanide Salts, *Corros. Sci*., **43**: 157–170 (2001).

[24] Halambek J., Cvjetko Bubalo M., Radojčić Redovniković I., Berković K., Corrosion Behaviour of Aluminum and AA5754 Alloy in 1% Acetic Acid Solution in Presence of Laurel Oil, *Int. J. Electrochem. Sci*., **9**: 5496 – 5506 (2014).

[25] Adejo S. O. and Ekwenchi M. M., Proposing a New Empirical Adsorption Isotherm known as Adejo-Ekwenchi Isotherm, *J. of Appl. Chem*., **6**(5): 66-71 (2014).

[26] Umoren S.A., Li Y., Wang F.H., Electrochemical Study of Corrosion Inhibition and Adsorption Behavior for Pure Iron by Polyacrylamide in H_2SO_4: Synergistic Effect of Iodide Ions, *Corros. Sci*., **52**: 1777–1786 (2010)

[27] Eddy N. O. and Mamza P. A. P., Inhibitive and Adsorption Properties of Ethanol Extract of Seeds and Leaves of Azardirachta Indica on the Corrosion of Mild Steel in H_2SO_4, *Portugal. Electrochim. Acta*, **27**(4): 443-456 (2009).

[28] Umoren, S. A.; Obot, I. B. and Igwe, I. O., Synergistic Inhibition between Polyvinylpyrollidone and Iodide Ions on Corrosion of Aluminum in HCl, *The Open Corrosion Journal*, **2**: 1-5 (2009).

[29] Popova A., Christov M., Vasilev A. and Zwetanova A., Mono-and Dicationic Benzothiazolic Quaternary Ammonium Bromides as Mild Steel Corrosion Inhibitors. Part I: Gravimetric and Voltammetric Results, *Corros. Sci.*, **53**: 679-680 (2011).

[30] Daoud D., Douadi T., Issaadi S., Chafaa S., Adsorption and Corrosion Inhibition of New Synthesized Thiophene Schiff Base on Mild Steel X52 in HCl and H_2SO_4 Solutions, *Corros. Sci.* **79:** 50–58 (2014).

[31] Branzoi V., Branzoi F., Baibarac M., The Inhibition of the Corrosion of Armco iron in HCl Solutions in the Presence of Surfactants of the Type of N-Alkyl Quaternary Ammonium Salts, *Mater. Chem. Phys.*, **65**: 288−297 (2000).